PERGAMON

Solid-State Electronics 45 (2001) 1121–1125

SOLID-STATE ELECTRONICS

Spontaneous oscillations and triggered pulsing in GaAs/InGaAs multiquantum well structures

A.G.U. Perera [a,*], S.G. Matsik [a], V.Y. Letov [a], H.C. Liu [b], M. Gao [b], M. Buchanan [b], W.J. Schaff [c]

[a] *Department of Physics and Astronomy, Georgia State University, Atlanta, GA 30303, USA*
[b] *Institute for Microstructural Sciences, National Research Council, Ottawa Canada, K1A 0R6*
[c] *School of Electrical Engineering, Cornell University, Ithaca, NY 14853, USA*

Received 7 December 2000; received in revised form 10 February 2001; accepted 23 February 2001

Abstract

Spontaneous and triggered pulsing behavior in InGaAs multiquantum well devices driven by a constant bias voltage are reported. Bias regions for the occurrence of spontaneous periodic oscillations as well as damped triggered pulsing were experimentally determined. An empirical model based on the observed shape of the *I–V* curve and the negative differential conductance is proposed to qualitatively explain both the triggered pulsing and the spontaneous oscillating behavior, which could lead to novel infrared detection techniques and neural network applications. © 2001 Elsevier Science Ltd. All rights reserved.

Keywords: Pulsing devices; InGaAs quantum well devices; Nonlinear effects; s-Type negative differential conductivity; Artificial neurons

Spontaneous pulsing has been observed at cryogenic temperatures in circuits containing silicon p^+–n–n^+ structures driven by a constant voltage [1] or a constant current source [2]. The circuits displayed a rich spectrum of both basic physics phenomena and applications. Interesting physics/nonlinear dynamics issues that have been studied using these phenomenon include the observation of Farey fractions, mode locking, and the transition to chaos [3]. Variation in the pulsing frequency with incident radiation led to these structures functioning as long wave infrared detectors [3] without preamplifiers. These structures in circuits have been used as basic logic gates. A circuit using the pulsing structures was used to detect a transient optical signal as in the case of the horseshoe crab eye simulating biological neurons [3]. The p^+–n–n^+ structures were treated as the artificial neurons, and the pulses were the action potentials as in the case of biological systems. Based on these similarities, following the architecture and signal transmission and processing of the primate retina [4] a parallel processor was proposed [3]. A single channel of this processor was formed to simulate a photoreceptor channel in a biological retina by using a filter circuit to combine two pulsing structures in series [4]. With suitable interconnections among channels, the multichannel circuit functioned as a parallel processor.

The use of p^+–n–n^+ structures in pulsing applications was limited to 4.2 K operation due to the low temperature at which the pulsing occurs. Obtaining spontaneous pulsing at higher temperatures would lead to expanded possibilities for the use of pulsing phenomena in various applications mentioned before. Study of oscillations in quantum well structures may lead to useful ideas towards increasing the operating temperature of pulsing structures. Current oscillations due to variations in the field domains have been observed in superlattices [5] and the effects of varying the drive amplitude on the oscillation pattern were studied. Oscillations were also observed under IR illumination [6]. The Gunn-like

* Corresponding author. Tel.: +1-404-651-2279; fax: +1-404-651-1427.
E-mail address: uperera@gsu.edu (A.G.U. Perera).

PII: S0038-1101(01)00138-1

Nomenclature

I	current (A)	τ_i	internal time constant (s)
V	voltage (mV)	R_L	load resistance (Ω)
V_C	output voltage (mV)	C_L	load capacitance (pF)
t	time (s)		

oscillations in superlattices while interesting in their own right are not readily useful in applications due to the high dc component in the current. This will be a characteristic of any device in which the variation in the current is smaller than the average current. In this paper, spontaneous and triggered pulsing behavior using a different mechanism based on the presence of s-type negative differential conductivity (NDC) in GaAs/InxGa$_{1-x}$As multiquantum well (MQW) structures is reported.

The MBE grown MQW device consists of 338 Å GaAs barriers and 83 Å $In_{0.087}Ga_{0.913}As$ wells as shown in Fig. 1. The structure consisted of 20 periods and the first and last barriers between the contacts and the wells at each end of the MQW region were 423 Å thick. The contacts were doped with Si to 1×10^{18} cm^{-3}, and the wells were δ-doped with Si to 4.0×10^{10} cm^{-2}. Based on these parameters the ground and first excited state energies would be expected at 24 and 59.5 meV giving a transition energy of 35 meV which is close to the optical phonon energy. A designed barrier height of 56.5 meV leads to a bound-to-continuum transition. The GaAs/InGaAs MQW structures were fabricated by etching 240 μm × 240 μm mesas using conventional wet chemical etching techniques. Ni/Ge/Au ohmic contacts were evaporated onto the top and bottom layers. The key feature of the 4.2 K dark I–V curve, as shown in Fig. 2 is the s-type NDC region between 0.436 and 0.459 V bias. A second smaller NDC region exists between 0.437 and 0.439 V bias. The dotted lines indicate the different regions: A ($I > 0.73$ mA), B ($0.66 < I <$ 0.73 mA), C ($0.60 < I < 0.66$ mA), D ($0.33 < I <$ 0.60 mA) and E ($I < 0.33$ mA) used to discuss the pulsing behavior. Regions B (0.436–0.438 V) and D (0.436–0.459 V) correspond to the smaller and larger bias ranges for negative differential conductance respectively. As the temperature is increased from 4.2 K the bias range of the negative differential conductance region is reduced and above 30 K the s-type feature disappears. Under bias variations the positive slope branches (regions A, C and E) remain stable while the negative slope branches (regions B and D) become unstable. Due to the instability of the constant bias condition, constant current was used for the I–V measurements. Although the cause of NDC region is an important issue to understand in order to design these pulsing structures, it is not the focus of this paper. However, the s-type shape may be due to impact ionization in combination with barrier lowering at the injection contact or could be due to phonon effects. The location of the excited state may play a significant role in determining whether s-type NDC is observed. A second similar structure except for a bound excited state did not show s-type NDC. The two branches of the s-type shape may be related to the relaxation of conduction electrons in the well. If the standard relaxation path is to the

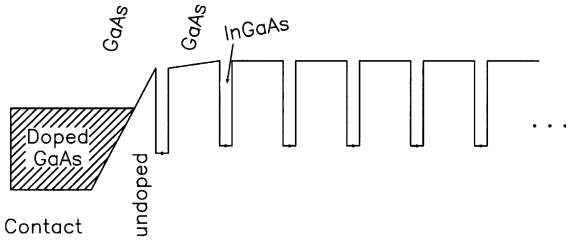

Fig. 1. Structure designed for the GaAs/InGaAs MQW device. The 338 Å thick barriers were GaAs and the 83 Å wells had an In fraction of 0.087 δ-doped to 4×10^{10} cm^{-2} with Si. The first and last barriers between the wells and the contacts were 423 Å thick and the contacts were Si doped to 1×10^{18} cm^{-3}.

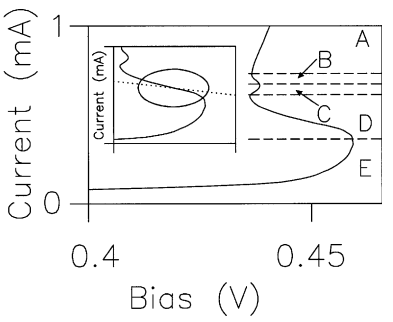

Fig. 2. Current–voltage curve for the device taken at 4.2 K showing the s-type negative differential resistance. The curve was measured under constant current conditions to avoid oscillations on the unstable branches. The various regions of different current stability and pulsing behavior are separated by dashed lines and labeled A through E. Regions B and D correspond to unstable current and spontaneous pulsing. Regions A, C, and E correspond to stable current and triggered pulses. The inset shows the load line (dotted line) and the path traced out by the device bias and current during a pulse (heavy line).

ground state, electrons would need to be re-excited before contributing to the conduction. However, if the relaxation was to the excited state the electrons could immediately enter the next barrier leading to increased conduction corresponding to the upper branch. This cause for the s-type shape would allow the design of structures operating at higher temperatures by increasing the barrier height and decreasing the well width. An additional possible source of s-type behavior is electron excitation into the X-band increasing transmission through AlAs barriers [7]. The use of X-band conduction could allow devices working at much higher temperatures.

The circuit used for the experiments is shown in Fig. 3. The steady state current is determined for the circuit from the intersection of the load line (current through the load resistor as a function of the pulsing device bias for a fixed total resistance) and the I–V curve. As the total bias on the circuit is varied, different types of current behavior are observed. When the load line intersects the I–V curve on an unstable branch (regions B and D in Fig. 2) the steady state current can be in an unstable equilibrium. Under these conditions a spontaneous periodic oscillation develops due to the small variations in the circuit current. When the load line crosses the I–V curve on one of the stable branches (regions A, C, and E) the current remains constant unless damped pulses are triggered by a small (~5 mV in this case) input pulse.

The oscillating behavior can be explained using a simple model based on the experimentally determined I–V characteristic. The model is similar to that used to explain bistability in resonant tunneling structures [8] with one significant difference. For resonant tunneling devices all branches of the device I–V are stable so that the instantaneous current always lies on the device I–V curve. For the device shown the negative conductivity branch is unstable which means that the instantaneous device current does not follow the device I–V curve.

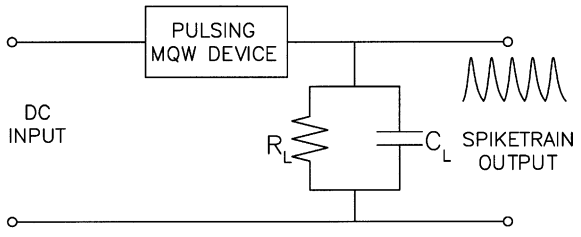

Fig. 3. The circuit used for the spiketrain generation. The input was a constant voltage source. In the case of spontaneous pulsing only the dc bias is present. A small spike was introduced by inductive coupling of a square wave for the observation of triggered oscillations. The load capacitance used was 500 pF and the load resistance 10 kΩ.

When the device current is not on the I–V curve the rate of change in current is given by

$$\frac{dI}{dt} = \Delta I/\tau_i, \tag{1}$$

where ΔI is the difference between the instantaneous current value and the steady state current closest to the instantaneous current at the instantaneous device bias, and τ_i is an internal time constant chosen to fit the pulse shape. The output voltage (V_C) is then found by solving

$$\frac{dV_C}{dt} = \frac{I}{C_L} - \frac{V_C}{R_L C_L}. \tag{2}$$

The solutions for V_C obtained from this differential equation with a constant capacitance and load resistance as well as the experimental oscillations are shown in Fig. 4. The simplest regions to explain are the unstable regions B and D in which spontaneous oscillations form. The instantaneous current and bias on the MQW device travels counterclockwise around a loop around the steady state point on the I–V curve as seen in the inset to Fig. 2. As the total applied bias is increased from 5.2 to 6.4 V with a load capacitance of 500 pF and resistance of 10 kΩ the frequency changes from 2.8 to 3.4 MHz. The amplitude of the oscillations, ~11 mV in region B and ~65 mV in region D appears to be related to the extent of the negative differential resistance region with larger regions producing larger oscillations. The amplitude of the oscillations does not equal the amplitude of the s-type region as there is overshoot at both ends while the device relaxes to the new current branch. There is a large dc current present in the circuit in addition to the oscillations which produces a constant voltage drop across the load resistor of 5–7 V depending on the overall circuit bias. The zero point of the curve has been adjusted

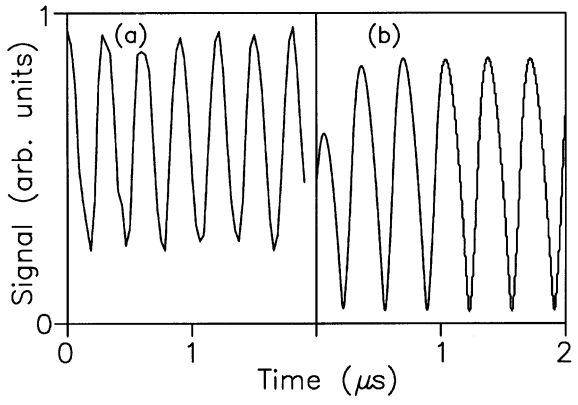

Fig. 4. (a) Experimental spontaneous oscillating response when the load line intersects the unstable branch for a total circuit bias of 7.18 V corresponding to region B. The capacitance is 544 pF and the load resistance is 10.1 kΩ. (b) Results of the model showing similar behavior.

to reduce the constant voltage in Fig. 4. The internal time constant in the model was chosen as 80 ns to give a reasonable agreement with the pulse widths observed. Increasing τ_i increases the width of the pulse for fixed capacitance and resistance. When triggered by an external source a pulse occurs for regions A and E. For biases near the transitions to regions B and D the pulse can be caused by the internal noise of the circuit as shown in Fig. 5. The level of noise needed to produce the pulsing decreases as the device bias becomes nearer to the transition value. In region C the duration of the triggered pulses depend on the amplitude of the triggering pulse and the device bias. If the trigger is <5 mV for biases above 0.438 V, damped oscillations will occur as in regions A and E, below 0.438 V bias, continuous oscillations occur as in regions B and D. Although relatively simple in its approach to determining the rate of change in current when the device is off the *I–V* curve, this model provides a reasonable qualitative agreement with the experimental results. Some deviation from the model is seen in the transitions between spontaneous and triggered pulsing behavior. While the model predicts the transitions to occur where the *I–V* changes from unstable to stable, experimentally triggered behavior has been observed for device biases between 0.45 and 0.46 where the *I–V* is unstable. This difference in stability of the current is probably due to the load resistance being large enough to cause the circuit to behave in a constant current mode. Changing the value of the load resistance should change the current at which the stability changes. The model also does not provide accurate values for the amplitude of the pulses. A detailed model for the current behavior connecting the device and circuit parameters will be the next step in order to design quantum well structures for pulsing at higher temperatures. Such a model will need to concentrate on determining the details of the rate of change of the nonsteady state current in order to explain the details of the pulsing behavior quantitatively.

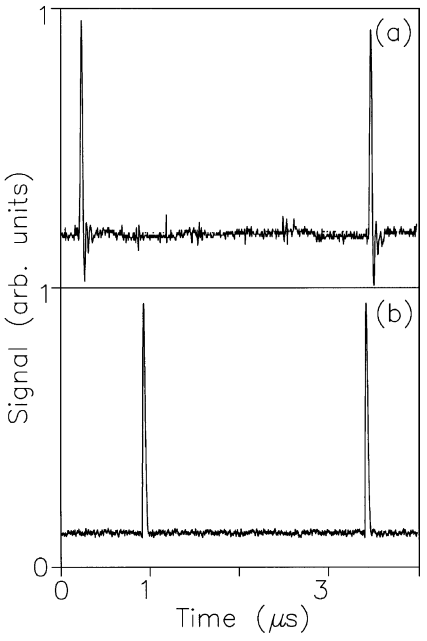

Fig. 5. (a) Experimental and (b) modeled triggered pulsing for device bias near the transition from lower stable branch to the unstable branch. The device pulses on an irregular pattern triggered by noise in the circuit. The capacitance and load resistance are the same as in the previous figure.

This device also functioned as a regular QWIP detector with response up to 35 μm for biases less than 0.235 V [9]. The peak responsivity for the detector was 0.45 A/W and the peak responsivity was 6.0×10^9 $\mathrm{cm}\sqrt{\mathrm{Hz}}/\mathrm{W}$ and NEP of 4.0×10^{-12} $\mathrm{W}/\sqrt{\mathrm{Hz}}$. The presence of both pulsing and IR response indicates the possibility of designing devices for pulsing mode detection [10]. The key concern in improving behavior of the device both as a detector and a pulsing generator will be to decrease the dark current. Improved dark current will probably involve reduced impurities in the structure.

In conclusion, oscillations have been observed in InGaAs quantum well structures at 4.2 K based on experimental data pulsing will continue up to 30 K. Both spontaneous periodic oscillations and triggered damped pulsing have been observed. The various types of pulsing behavior have been connected to the shape of the *I–V* curve. A simple model based on the s-type NDC in the *I–V* curve has been developed to give a qualitative explanation of the pulsing behavior. Further research into origin of the s-type behavior could lead to pulsing being obtained at higher temperatures. In particular, increasing in the barrier height by increasing the In fraction or using AlGaAs barriers could lead to pulsing at higher temperatures.

Acknowledgements

This work was supported in part by the NSF under grant #ECS-98-09746. The work at NRC was supported in part by DND. The authors wish to thank Dr. A. Korotkov for helpful discussions at the early stages of this work.

References

[1] Coon DD, Ma SN, Perera AGU. Farey-fraction frequency modulation in the neuronlike output of silicon p-i-n diodes at 4.2 K. Phys Rev Lett 1987;58(11):1139–42.

[2] Coon DD, Perera AGU. Integrate-and-fire coding and Hodgkin-Huxley circuits employing silicon diodes. Appl Phys Lett 1989;55(5):478–80.

[3] Perera AGU. Physics and novel device applications of semiconductor homojunctions. In: Francombe MH, editor. The physics of thin films, vol. 21. San Diego: Academic Press; 1995. p. 1–75.
[4] Perera AGU, Betarbet SR, Matsik SG. Bifurcations and chaos in pulsing Si neurons. World Congress on Neural Networks (WCNN 94 San Diego), vol. IV, Hillsdale, NJ: Lawrence Erlbaum Associates; 1994. p. 704–9.
[5] Luo KJ, Ploog KH, Bonilla LL. Explosive bifurcation to chaos in weakly coupled semiconductor superlattices. Phys Rev Lett 1998;81(6):1290–3.
[6] Luo KJ, Teitsworth SW, Kostial H, Grahn HT, Ohtani N. Controllable bistabilities and bifurcations in a photoexcited GaAs/AlAs superlattice. Appl Phys Lett 1999; 74(25): 3845–7.
[7] Belyantsev AM, Romanova YuYu. Intervalley mechanism for the formation of s-type negative differential conductivity in short heterostructures. Semiconductors 1995;29(8): 781–2.
[8] Liu HC. Circuit simulation of resonant tunneling double-barrier diode. J Appl Phys 1988;64(9):4792–4.
[9] Perera AGU, Matsik SG, Liu HC, Gao M, Buchanan M, Schaff WJ, Yeo W. GaAs/InGaAs quantum well infrared photodetector with a cutoff wavelength at 35 μm. Appl Phys Lett 2000;77(5):741–3.
[10] Coon DD, Perera AGU. Mode locked infrared sensors. Appl Phys Lett 1987;51(14):1086–8.